Int J Earth Sci (Geol Rundsch) (2017) 106:1631–1649
DOI 10.1007/s00531-016-1375-3

ORIGINAL PAPER

The timing of metamorphism in the Odenwald–Spessart basement, Mid-German Crystalline Zone

T. M. Will[1] · B. Schulz[2] · E. Schmädicke[3]

Received: 7 March 2016 / Accepted: 6 July 2016 / Published online: 18 July 2016

Abstract New in situ electron microprobe monazite and white mica $^{40}Ar/^{39}Ar$ step heating ages support the proposition that the Odenwald–Spessart basement, Mid-German Crystalline Zone, consists of at least two distinct crustal terranes that experienced different geological histories prior to their juxtaposition. The monazite ages constrain tectonothermal events at 430 ± 43 Ma, 349 ± 14 Ma, 331 ± 16 Ma and 317 ± 12 Ma/316 ± 4 Ma, and the $^{40}Ar/^{39}Ar$ analyses provide white mica ages of 322 ± 3 Ma and 324 ± 3 Ma. Granulite-facies metamorphism occurred in the western Odenwald at c. 430 and 349 Ma, and amphibolite-facies metamorphism affected the eastern Odenwald and the central Spessart basements between c. 324 and 316 Ma. We interpret these data to indicate that the Otzberg–Michelbach Fault Zone, which separates the eastern Odenwald–Spessart basement from the Western Odenwald basement, is part of the Rheic Suture, which marks the position of a major Variscan plate boundary separating Gondwana- and Avalonia-derived crustal terranes. The age of the Carboniferous granulite-facies event in the western Odenwald overlaps with the minimum age of eclogite-facies metamorphism in the adjacent eastern Odenwald. The granulite- and eclogite-facies rocks experienced contrasting pressure–temperature paths but occur in close spatial proximity, being separated by the Rheic Suture. As high-pressure and high-temperature metamorphisms are of similar age, we interpret the Odenwald–Spessart basement as a paired metamorphic belt and propose that the adjacent high-pressure and high-temperature rocks were metamorphosed in the same subduction zone system. Juxtaposition of these rocks occurred during the final stages of the Variscan orogeny along the Rheic Suture.

Keywords Odenwald–Spessart basement · Mid-German Crystalline Zone · Terrane boundary · In situ monazite age dating · $^{40}Ar/^{39}Ar$ age data · Paired metamorphic belt

Introduction

The Mid-German Crystalline Zone is a several hundred kilometres long, NE–SW striking belt of medium- to high-grade Variscan basement outcrops, which separate unmetamorphosed and low-grade rocks of the Rhenohercynian Northern Phyllite Zones in the northwest from low- to medium-grade rocks of the Saxothuringian Zone in the southeast (Fig. 1). The Mid-German Crystalline Zone is thought to have formed during the late Variscan closure of the Rheic Ocean that had previously separated Gondwana from Laurussia (i.e. Laurentia, Avalonia and Baltica). Rocks representing the Avalonian microplate, that already split from Gondwana in the Upper Cambrian to Lower Ordovician (e.g. Linnemann et al. 2007), occur to the north of the Mid-German Crystalline Zone, whereas the former Gondwana margin lies to its south. Thus, the associated Variscan plate boundary or suture (Rheic Suture) should be located within the Mid-German Crystalline Zone (e.g.

Electronic supplementary material The online version of this article (doi:10.1007/s00531-016-1375-3) contains supplementary material, which is available to authorized users.

✉ T. M. Will
thomas.will@uni-wuerzburg.de

[1] Institut für Geographie und Geologie der Universität Würzburg, Am Hubland, 97074 Würzburg, Germany

[2] Institut für Mineralogie, TU Bergakademie Freiberg, Brennhausgasse 14, 09596 Freiberg, Germany

[3] GeoZentrum Nordbayern, Universität Erlangen-Nürnberg, Schlossgarten 5a, 91054 Erlangen, Germany

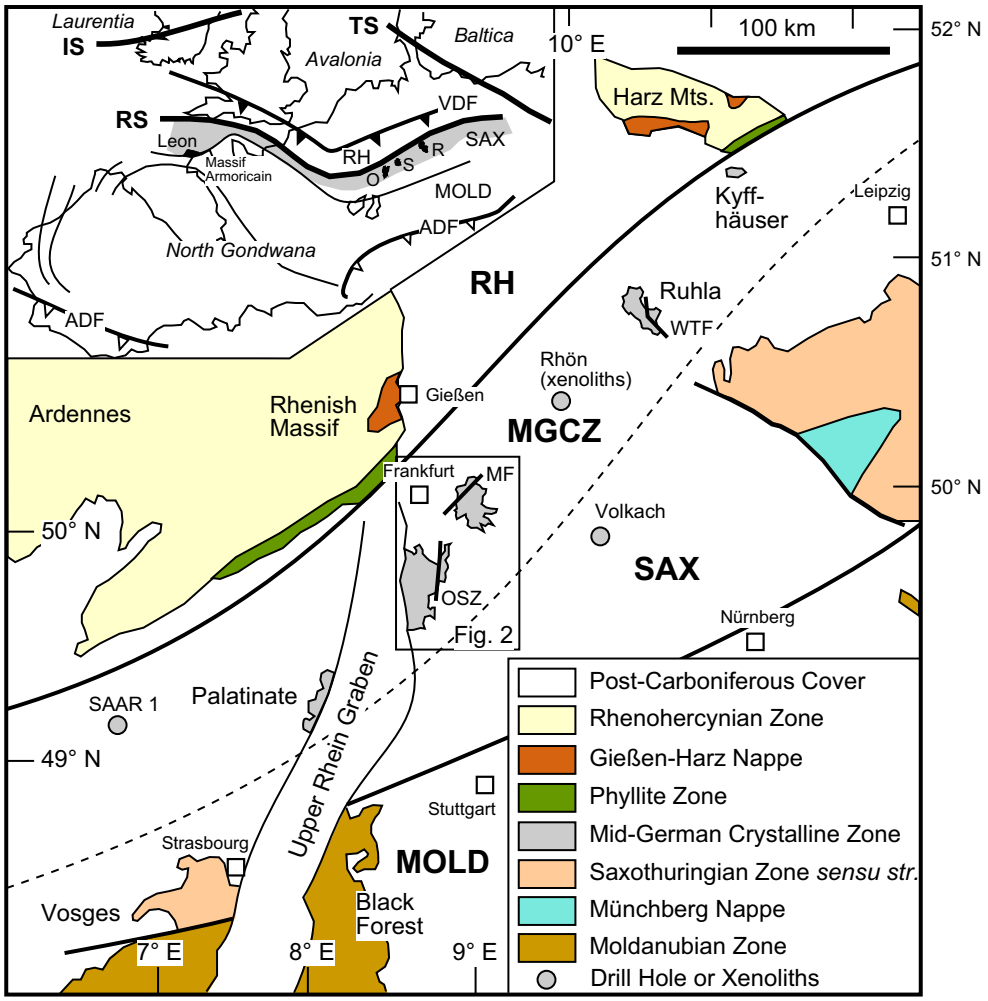

Fig. 1 Location of the Mid-German Crystalline Zone (MGCZ) in Central Europe (modified after Will et al. 2015). RH, Rhenohercynian Zone; SAX, Saxothuringian Zone; MOLD, Moldanubian Zone; only the exposed areas are shown on the map. Additional abbreviations in *inset*: IS, Iapetus Suture; TS, Tornquist Suture; RS, Rheic Suture; VDF, Variscan deformation front; ADF, Alpine deformation front; MF, Michelbach Fault; OSZ, Otzberg Shear Zone; WTF, West Thuringian Fault; O, Odenwald; S, Spessart; R, Rhön

Oncken 1997; Zeh and Gerdes 2010; Will et al. 2015). For a more complete summary of the geological setting of the Mid-German Crystalline Zone see Zeh and Will (2010).

The Odenwald–Spessart basement forms the largest part of the exposed Mid-German Crystalline Zone in Germany (Fig. 2). Based on new lithogeochemical and Sr–Nd–Pb isotope data, Will et al. (2015) concluded that the Odenwald–Spessart basement consists of two distinct crustal terranes that are tectonically separated by the Otzberg–Michelbach Fault Zone. The petrogenesis of the pre-metamorphic oceanic mafic protoliths comprising ocean ridge, intraplate and arc-derived metabasaltic rocks and the metamorphic conditions of the basement are reasonably well known (Will 1998; Will and Schmädicke 2001, 2003; Marx 2008; Will et al. 2015). However, direct geochronological constraints on the age of metamorphism are sparse (see below). To fill this gap, we present new geochronological data for low- to high-grade schist and gneiss from the Odenwald–Spessart basement. The main method was in situ U–Th–Pb electron microprobe dating of monazite, but a few ages were determined by white mica $^{40}Ar/^{39}Ar$ step heating experiments. The former method was used because it provides a direct link between monazite growth and the age of metamorphism on the condition that monazite growth can be linked to a particular mineral assemblage (e.g. metamorphic peak or retrograde mineral assemblages). The age of (peak) metamorphism may differ across the area, which, however, is to be expected if the basement is made up of two crustal terranes that experienced different geological histories prior to their juxtaposition in the Upper Carboniferous.

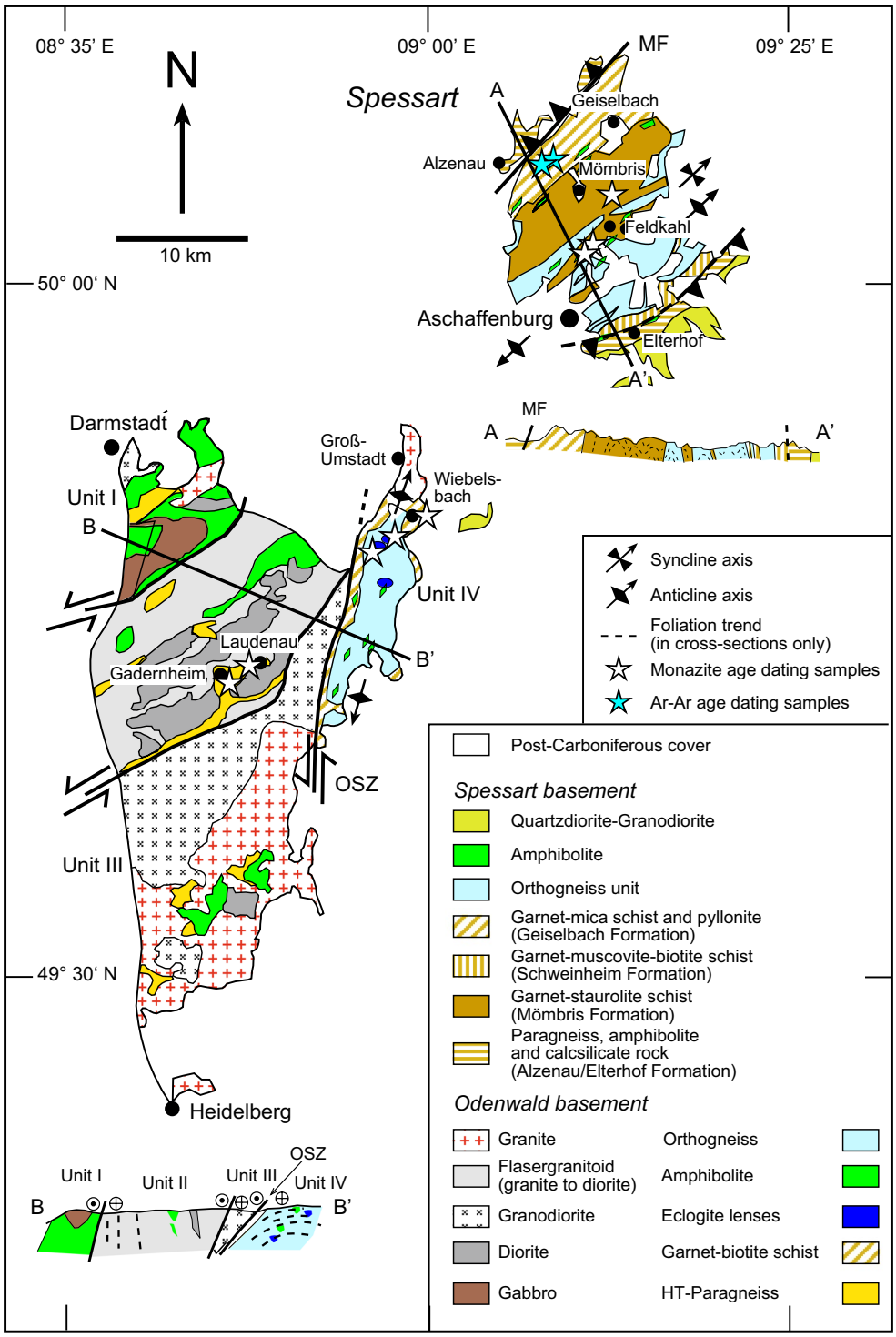

Fig. 2 Geological map of the Odenwald–Spessart basement (modified after Will et al. 2015). OSZ, Otzberg Shear Zone; MF, Michelbach Fault. The sample locations are indicated by the *stars* (*white star* EMP monazite growth age, *blue star* $^{40}Ar/^{39}Ar$ white mica age)

Regional background

Odenwald basement

The Odenwald consists of two fundamentally different basement units that are separated by the NNE–SSW trending Otzberg Shear Zone (Fig. 2), a steeply westerly dipping semi-brittle to ductile fault and shear zone with a transtensional sinistral strike-slip sense of shear (Krohe 1992; Will 2001). The basement of the western Odenwald (units I to III sensu Krohe 1992) is dominated by large quantities of calc-alkaline magmatic rocks that occupy some 90 vol% of the entire outcrop area (Altherr et al. 1999; Okrusch et al. 2000). Compositionally, these rocks range from granite to gabbro that were emplaced at 362 ± 9 Ma in the north (Kirsch et al. 1988) and some 30 myr later further south (Siebel et al. 2012). Subordinate amphibolite-facies metabasic rocks and high-temperature, low-pressure granulite and migmatitic gneiss also occur in the western Odenwald (e.g. von Raumer 1973). Zircon fusion ages of 342–332 Ma, which overlap with hornblende $^{40}Ar/^{39}Ar$ cooling ages of amphibolite (Schubert et al. 2001), were interpreted as the time of high-temperature metamorphism and partial melting in the southern Odenwald (units II and III) by Todt et al. (1995). The core of the eastern Odenwald (unit IV) consists mainly of S-type granitic to granodioritic orthogneisses of supposed volcanic arc origin (Altenberger and Besch 1993). The orthogneiss protoliths intruded at c. 410–405 Ma (Reischmann et al. 2001) and are interpreted to form a NNE–SSW trending antiform with fold axes that plunge c. 10° NNE (Chatterjee 1960). In addition, slivers of variably deformed amphibolite, metagabbro and ultramafic rock as well as garnet–amphibolite are present in the eastern Odenwald (Knauer et al. 1974; Nickel 1975). Garnet–amphibolite within the succession has been recognised as retrogressed eclogite that initially formed during high-pressure, subduction-related metamorphism (Will and Schmädicke 2001) of depleted mid-ocean ridge basalt (Will et al. 2015). A metapsammitic garnet-bearing biotite schist unit, also referred to as 'schist envelope', crops out at several locations around the Odenwald orthogneiss core and is closely associated with the Otzberg Shear Zone. Todt et al. (1995) proposed that granitic magmas intruded the schist unit before or close to the end of the thermal peak of metamorphism in the eastern Odenwald, which, according to these authors, occurred at 375 ± 5 Ma. However, this interpretation is questionable because of the c. 30-myr-old granitoid intrusion ages determined by Reischmann et al. (2001) and the Lower Carboniferous amphibolite-facies metamorphism of the schist unit (this study, see below). Thus, it is conceivable that the zircon fusion ages of Todt et al. (1995) are mixing ages.

The eclogite-facies metabasic rocks in the eastern Odenwald are characterised by clockwise pressure–temperature (*P–T*) paths, with peak conditions of some 700 ± 50 °C at minimum pressures of 16–17 kbar (Will and Schmädicke 2001). In contrast, the granulite-facies paragneiss in the western Odenwald followed a hairpin-like, counterclockwise *P–T* path at maximum pressures of 4 kbar and minimum temperatures of c. 680 °C (Will and Schmädicke 2003). These authors interpreted the high-pressure eclogites and the adjacent, low-pressure/high-temperature granulites as a paired metamorphic belt above a west-directed subduction zone (in present-day coordinates). A minimum age of 357 ± 6 Ma was determined for the eclogite-facies event (Scherer et al. 2002). The age of the granulite-facies metamorphism is currently unknown.

Spessart basement

The Spessart basement (Fig. 2) is interpreted as a c. 25-km-wide, NE trending asymmetric antiform (Weber 1995). The central part of the Spessart basement is made up of medium-grade garnet-staurolite schist and paragneiss with rare kyanite and/or sillimanite (Mömbris Formation), mica schist and phyllonite that locally contain pseudomorphs after garnet (Geiselbach Formation), and a well-foliated calc-alkaline granitic to granodioritic orthogneiss unit with a Upper Silurian to Lower Devonian intrusion age of 418–410 ± 18 Ma (Dombrowski et al. 1995). In addition, garnet- and rarely also garnet-staurolite-bearing biotite-muscovite schist (Schweinheim Formation) is exposed in the south of the Spessart basement. The Alzenau Formation in the northernmost and the Elterhof Formation in the southernmost parts of the Spessart basement are composed of variably deformed granitic gneiss, quartzite, marble, calc-silicate rock, garnet-bearing biotite gneiss and minor amphibolite. In addition, the Elterhof Formation was intruded by weakly deformed quartzdiorite and granodiorite at c. 330 Ma (Anthes and Reischmann 2001; Siebel et al. 2012). The Spessart basement experienced amphibolite-facies metamorphism with peak temperatures of c. 600–670 °C at 8–10 kbar during the Carboniferous (Will 1998; Marx 2008; Zeh and Will 2010). The age of peak metamorphism is unknown but some K–Ar, Ar–Ar and Rb–Sr age data of metamorphic minerals in felsic and mafic lithologies provide evidence that the basement cooled from temperatures in excess of c. 500 °C to below 300 °C between 328 and 311 Ma (Lippolt 1986; Nasir et al. 1991; von Seckendorff et al. 2004). Upper Carboniferous deformational and thermal events are not only recognised in the Odenwald–Spessart basement but are well known from many locations in the central European Variscides, where deformation, amphibolite-facies metamorphism, granitoid intrusions and anatexis occurred between c. 330 and 315 Ma (e.g. summary in Kroner and Romer 2013).

Variscan terrane boundaries in the Odenwald–Spessart basement

Several authors suggested that the basement rocks in the Mid-German Crystalline Zone can be assigned to different tectonostratigraphic units (e.g. Oncken 1997; Altherr et al. 1999; Krohe 1992, 1996; Will 2001; Zeh and Gerdes 2010; Zeh and Will 2010). This view was recently substantiated by a geochemical and Sr–Nd–Pb isotope study of Odenwald–Spessart basement rocks (Will et al. 2015). These authors showed that the geochemical and isotope data of tholeiitic metabasic rocks from the northernmost part of the Spessart basement (Alzenau Formation) and the western Odenwald are almost identical, suggesting that their corresponding basements belong to the same tectonostratigraphic unit. Will et al. (2015) argued further that the protoliths of the Alzenau Formation and western Odenwald metabasic rocks might have formed in a back-arc setting. The poorly exposed Michelbach Fault (Fig. 2) separates the northernmost part of the Spessart basement from the central and southern Spessart basement. The protoliths of metabasic rocks south of the Michelbach Fault formed in either an intraplate oceanic island or a continental arc setting (Will et al. 2015). As a consequence, the Michelbach Fault and the Otzberg Shear Zone (see above) must be segments of the same zone of crustal weakness that separates the Odenwald and Spessart basements into two distinct crustal terranes. As a corollary, the previously held proposition that the Alzenau and the Elterhof Formations of the Spessart basement are relics of a once coherent lithological unit (e.g. Behr and Heinrichs 1987; Weber 1995) must be abandoned in the light of the new data presented by Will et al. (2015).

Thus, the combined Otzberg–Michelbach Fault Zone is interpreted to correspond to the position of a major Variscan terrane boundary between Gondwana- and Baltica/Avalonia-derived terranes in the Odenwald–Spessart basement (Will et al. 2015). In addition, the Spessart (except for the Alzenau Formation) and the eastern Odenwald basements represent a tectonic window of lower plate Baltica/Avalonia-derived rocks within the upper plate Gondwana-related terranes, with the Otzberg–Michelbach Fault Zone defining the western outcrop limit of the Spessart–eastern Odenwald tectonic window.

Results

$^{39}Ar/^{40}Ar$ step heating of white mica

White mica fractions from two garnet-bearing quartz-mica schist samples from the Geiselbach Formation in the central Spessart basement (abandoned quarry NE of the township of Hemsbach; Fig. 2) were dated with the $^{40}Ar/^{39}Ar$ technique. A summary of the samples analysed, the calculated ages and comments on the interpretation of the data is given in Table 1. All errors are given at the 1σ level. Stepwise heating of sample *Sp08-5* produced a plateau between steps 8 and 17 (78.4 % ^{39}Ar released), with a calculated plateau age of 325.2 ± 0.6 Ma (Fig. 3a). The inverse isochron age for these steps is 323.6 ± 3.4 Ma (Fig. 3b) and is identical to the weighted plateau age. Sample *Sp08-4* yielded a plateau between steps 12 and 18 (47.9 % ^{39}Ar released) with a weighted plateau age of 321.2 ± 1.2 Ma (Fig. 3c). An inverse isochron for these steps forced through the atmospheric $^{36}Ar/^{40}Ar$ ratio of 295.5 yields an age of 323.5 ± 1.7 Ma (Fig. 3d). Thus, the step heating experiments yielded undistinguishable results, with the preferred minimum ages for white mica crystallisation in samples *Sp08-5* and *Sp08-4* being 324 ± 3 Ma and 322 ± 3 Ma (L. Ratschbacher and J. Pfänder, pers. comm. 2016; see also caption to Table 1). The analytical procedures are summarised in "Appendix 1" and the complete step heating data are given in the Electronic Supplement Table S1.

Electron microprobe dating of monazite

Monazite that may crystallise either from peraluminous melts or due to metamorphic reactions appears as one of the most useful minerals to unravel the timing of tectonometamorphic events (do Couto et al. 2016). Depending

Table 1 $^{40}Ar/^{39}Ar$ ages of mica schists from the Geiselbach formation of the Spessart basement

Sample	Exp.Nr.	Mineral	weight (mg)	WMA [Ma]	MSWD	Steps	$\%^{39}Ar$	IIA	MSWD	$(^{40}Ar/^{36}Ar)_i$	Steps
Sp 08-4	2434	white mica	2.05	321.2 ± 1.2	1.17	12–18	47.9	–	–	–	–
Sp 08-5	2437	white mica	2.26	325.2 ± 0.6	0.53	8–17	78.4	323.6 ± 3.4	0.57	977 ± 590	8–17

All errors are 1σ. MSWD is the mean square weighted deviation. Inverse isochron age (IIA) and weighted mean age (WMA) are based on fraction of ^{39}Ar and steps listed. Preferred age interpretation: Sp 08-4 white mica: two isochrons with mixing between atmosphere and a radiogenic component of ~323 Ma and atmosphere and a radiogenic component of ≤137 Ma, preferred estimate of old component 322 ± 3 Ma; Sp 08-5 white mica: two isochrons with mixing between atmosphere and a radiogenic component of ~324 Ma and atmosphere and a radiogenic component of <264 Ma, preferred estimate of old component 324 ± 3 Ma. The determined ages correspond to the time at which the mineral cooled through the closure temperatures of c. 350 (e.g. Hodges 2003). However, given the fact that the quartz-mica schist samples were metamorphosed at lower amphibolite-facies conditions the determined age will be close to the time of peak metamorphism

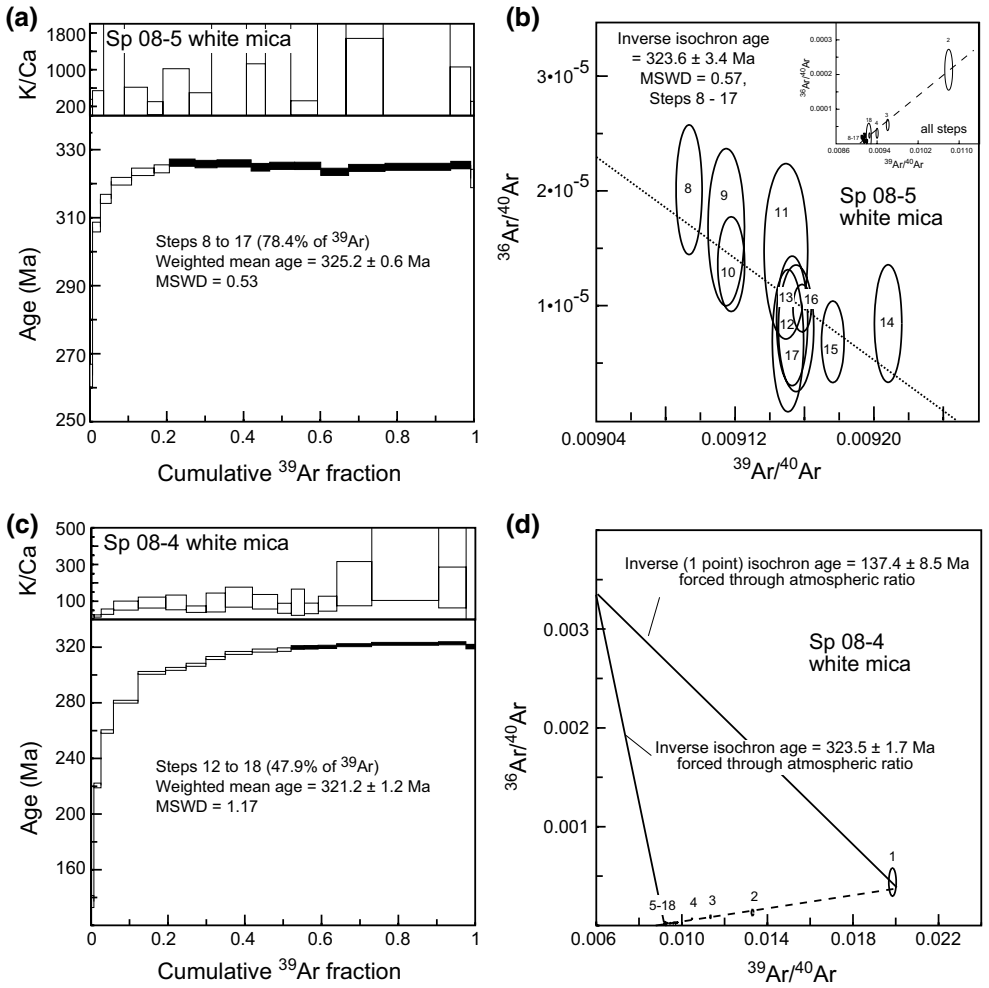

Fig. 3 **a**, **c** $^{40}Ar/^{39}Ar$ white mica age spectra and **b**, **d** inverse isochron diagrams for mica schist samples from the Geiselbach Formation, central Spessart basement

on bulk composition, monazite crystallises in Ca-poor and Al-rich metapelitic rocks under upper greenschist- to granulite-facies conditions and has a bulk closure temperature of c. 990 °C (Cherniak et al. 2002). Because of the extremely low diffusion rates of Pb in monazite, even at high temperatures (e.g. Cocherie and Albarède 2001) and the high closure temperature, the age determined of a metamorphic monazite is interpreted to indicate the time of crystallisation rather than cooling. The fact that monazite grains can be dated in situ by the electron microprobe (Montel et al. 1996) allows the determination of possible superimposed magmatic and/or metamorphic events if the original textural contacts of the measured monazite grains are preserved. As a consequence, monazite in situ dating provides an excellent technique for estimating the growth of metamorphic minerals and mineral assemblages in polymetamorphic terranes. Ages of monazite grains from 11 paragneiss and two orthogneiss samples of the Odenwald–Spessart basement (Table 2) were determined following the approaches outlined by Montel et al. (1996) and Suzuki et al. (1994), respectively. The results obtained by the two different methods coincide exceptionally well in all samples analysed (Fig. 4 and Electronic Supplement Table S2). Analytical details are summarised in "Appendix 2".

Textural characteristics of monazite grains

Monazite grains were identified by backscattered electron imaging (BSE) prior to electron microprobe analysis (EMP). With a few exceptions, the longest dimension of most monazite grains in the metasedimentary rocks of the eastern Odenwald–Spessart basement varies between 35 and 110 µm and is similar to those in the high-grade paragneiss of the western Odenwald basement (35–90 µm). The monazite grains in the orthogneiss host rock of the eastern Odenwald eclogite range from 35 to 140 µm in the metagranite sample EH 6 and from 70 to 360 µm in the metagranodiorite KK 7. Except for one grain in sample EH 6, no oscillatory zoning being indicative

Table 2 Sample location, description and results of in situ Th–U–Pb EMP monazite samples from the Odenwald–Spessart basement

Sample	Location	Mineral assemblage	Metamorphic peak conditions	Monazite characteristics (with reference to Fig. 5)	Number of analyses	Weighted average age ± 2σ (MSWD)	ThO_2^* versus PbO age (Ma)
Spessart basement							
Medium-temperature metapelitic schist							
Sp 6b Grt-st schist	Grauenstein R ^{35}11450 H ^{55}42000	grt(2–3), st, bi, mu. plag, qtz	~620 °C/6–7 kbar (own unpubl. data)	Xeno- to hypidiomorphic, ~35–85 μm, few grains are rounded, in matrix, wm and bi (Fig. 5a)	27	317 ± 20 Ma (0.057)	317
Sp 103 Grt-st schist	Grauenstein R ^{35}11300 H ^{55}41540	grt(2–3), st, bi, mu. plag, qtz	~620 °C/6–8 kbar (own unpubl. data)	Xenomorphic, 45–160 μm, few grains are rounded, in matrix and bi	9	316 ± 17 Ma (0.116)	317
Sp 1063 Grt-ky-st schist	Schimborn R ^{35}13300 H ^{55}47060	grt(2), st, bi, ky, sill, mu, plag, qtz, <chl	~650 ± 20 °C/9 ± 1 kbar (Will 1998; Marx 2008)	Xeno- to hypidiomorphic, ~50–115 μm, in matrix and bi (Fig. 5b)	8	319 ± 35 Ma (0.032)	319
				All metapelite data	44	317 ± 12 Ma (0.061)	317
Odenwald basement							
Eastern Odenwald (unit IV)							
Low- to medium-temperature metapsammitic schist ('schist envelope')							
Wi 2-2 Grt schist	Wiebelsbach R ^{34}96700 H ^{55}21375	grt(3–4), plag, bi, qtz	Greenschist- to lower amphibolite-facies	Xenomorphic to rounded 20–100 μm, locally fractured grains, in matrix and a few grains in bi	23	317 ± 11 Ma (0.117)	317
Wi 4a-1 Grt schist	Wiebelsbach R ^{34}96850 H ^{55}21350	grt(0.5), plag, bi, qtz	Greenschist- to lower amphibolite-facies	Xenomorphic to rounded 35–105 μm, locally fractured grains, in bi, qtz, matrix	17	316 ± 7 Ma (0.350)	314
Wi 4a-2 Grt schist	Wiebelsbach R ^{34}96850 H ^{55}21350	grt(1), plag, bi, qtz	Greenschist- to lower amphibolite-facies	Xeno- to hypidiomorphic ~35–75 μm, (a few grains up to 200 μm), locally fractured/rounded grains, in matrix and bi (Fig. 5c)	38	316 ± 5 Ma (0.120)	314
				All metapsammitic schist data	78	316 ± 4 Ma (0.200)	314

Table 2 continued

Sample	Location	Mineral assemblage	Metamorphic peak conditions	Monazite characteristics (with reference to Fig. 5)	Number of analyses	Weighted average age ± 2σ (MSWD)	ThO_2^* versus PbO age (Ma)
Orthogneiss (eclogite host rocks)							
EH 6 Grt-sp-bearing metagranite	Eierhöhe R ^{34}95600 H ^{55}19400	qtz, ksp, plag, <mu, ≪grt(0.5), ≪Zn-sp	Unknown	Xeno- to hypidiomorphic, 35–140 μm, in matrix, ksp and qtz	8	331 ± 28 Ma (0.075)	331
KK 7 Metagranodiorite	Klingelskopf R ^{34}94600 H ^{55}18600	qtz, plag, bi, <ksp	Unknown	Xenomorphic to rounded, 90–360 μm, few grains are rounded, in matrix, bi and qtz (Fig. 5d)	23	329 ± 19 Ma (0.061)	328
				All eclogite host rock data	31	331 ± 16 Ma (0.063)	331
Western Odenwald (unit II)							
High-temperature paragneiss near Laudenau							
LD 3 Sill-grt-crd paragneiss	Laudenau R ^{34}85700 H ^{55}08950	grt(5), sill, crd, plag, sp, <cor,	~680 °C/3.5 kbar (Will and Schmädicke 2003)	Xenomorphic, 35–85 μm, in matrix and grt	14	345 ± 30 Ma (0.061)	345
LD 7 Grt-sp-crd paragneiss	Laudenau R ^{34}85650 H ^{55}08900	grt(3), crd, sp, plag, <mu, <cor,	~680 °C/3.5 kbar (Will and Schmädicke 2003)	Xenomorphic to rounded, ~35–60 μm, in matrix and grt (Fig. 5e)	15	347 ± 30 Ma (0.079)	347
KG 316 Sill-crd-paragneiss	Klein-Gumpen R ^{34}86550 H ^{55}07800	sill, crd, sp, plag, bi	~680 °C/3–4 kbar	Xenomorphic, ~45–80 μm, in matrix (Fig. 5f)	28	351 ± 21 Ma (0.064)	350
OD 76 Sill-grt-crd paragneiss	Laudenau R ^{34}85600 H ^{55}08900	grt(15–20), sill, crd, bi, plag, sp (only as incl. in grt)	~680 °C/3–4 kbar	Xenomorphic to tabular, 50–75 μm, in grt (Fig. 5g)	5	356 ± 56 Ma (0.068)	357
				All Laudenau granulite data	62	349 ± 14 Ma (0.066)	350
High-temperature paragneiss near Gadernheim							
GH 4 Sill-qtz-grt-crd Paragneiss	Gadernheim R ^{34}82200 H ^{55}08700	grt(25–30), plag, crd, bi, sill, qtz	>640 °C/4–5 kbar (Will and Schmädicke 2003)	Hypidiomorphic to rounded, in matrix and grt, 70–90 μm (Fig. 5h)	6	430 ± 43 Ma (0.120)	431
				Gadernheim granulite data	6	430 ± 43 Ma (0.120)	431

ThO_2^* is the sum of ThO_2 measured and the ThO_2 equivalent to the UO_2 concentration measured. The weighted average age of the apparent individual spot ages, which were determined according to Montel et al. (1996), were calculated using Isoplot 3.70 (Ludwig 2008); MSWD—mean square weighted deviation. The ThO_2^* versus PbO ages were determined according to Suzuki et al. (1994). The approximate modal amount of garnet is given (in vol%) in parentheses

Preferred ages are in bold print

Mineral abbreviations: *grt* garnet, *ksp* K-feldspar, *plag* plagioclase, *bi* biotite, *qtz* quartz, *ky* kyanite, *sill* sillimanite, *crd* cordierite, *st* staurolite, *mu* muscovite, *sp* spinel, *cor* corundum

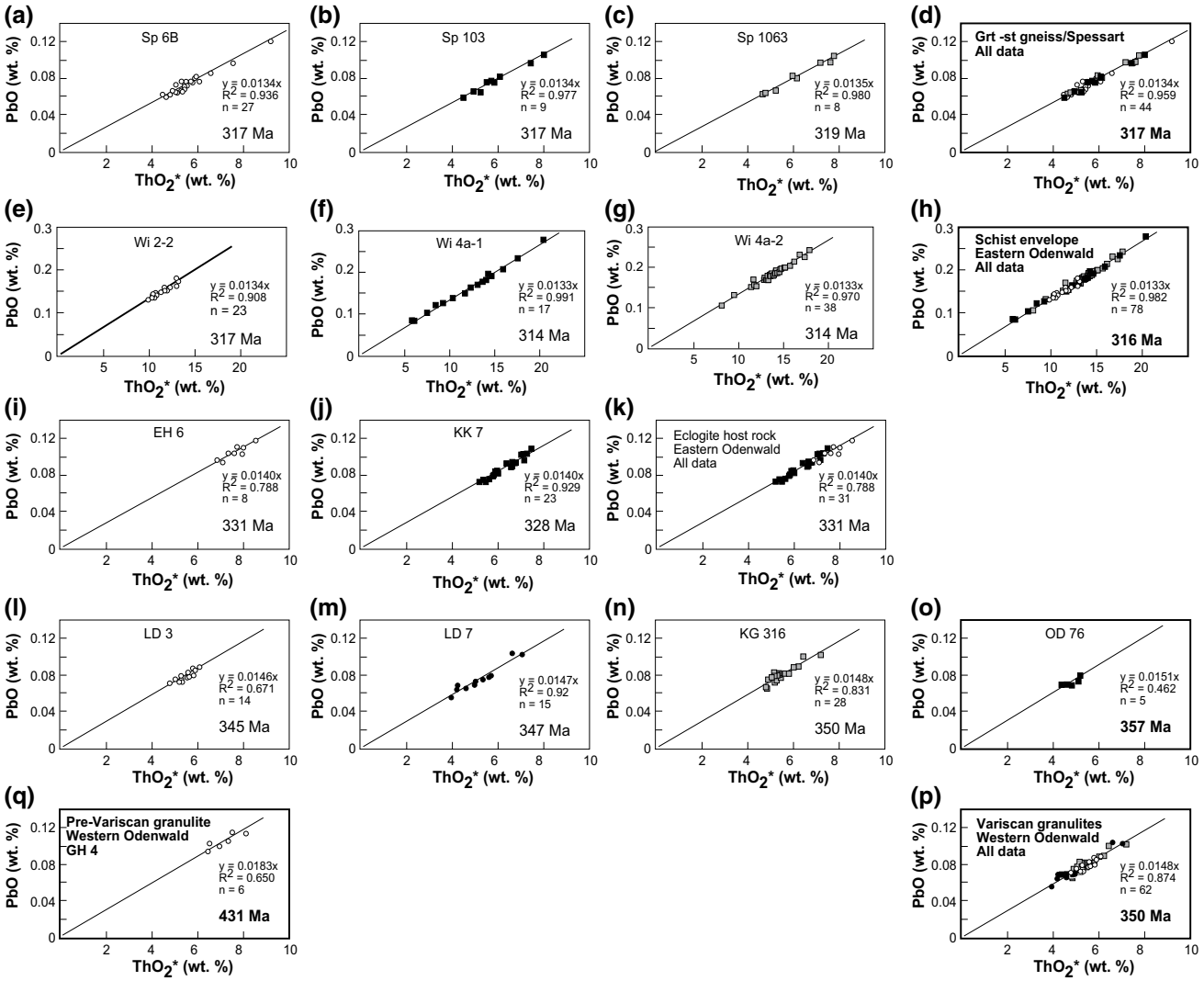

Fig. 4 ThO_2^* versus PbO isochron plots for monazite analyses obtained by in situ EMP monazite dating. The ages correspond to the slope of the regression lines (Suzuki et al. 1994); the weighted average ages and their 2σ standard deviations are given in Table 2 and the Electronic Supplement Table S2

of magmatic growth was observed in any of the several 100s of monazite grains investigated by BSE imaging. Instead, the mineral is typically characterised by homogeneous shades of grey without distinct zonation patterns and associated larger variations in ThO_2 contents (Electronic Supplement Table S2). In general, no correlation between grain size and metamorphic grade is obvious (Table 2).

Age of monazite growth in the eastern Odenwald–Spessart tectonic window (lower plate)

The textural positions of monazite grains used for in situ dating are exemplarily shown in Fig. 5. The amphibolite-facies garnet-staurolite paragneiss samples Sp 6b, Sp 103, and Sp 1063 from the Mömbris Formation in the central Spessart basement yielded Upper Namurian- to Lower Westphalian-weighted average ages of 317 ± 20 Ma, 316 ± 17 Ma and 319 ± 35 Ma, respectively (Table 2; Figs. 4a–c, 5a, b). Regressing all data ($n = 44$) gives an age of 317 ± 12 Ma for monazite growth (Table 2). Identical ages of 317 ± 11 Ma, 316 ± 7 Ma and 316 ± 5 Ma were obtained for three upper greenschist- to amphibolite-facies metapsammitic samples (Wi 2-2, Wi 4a-1 and Wi 4a-2) of the eastern Odenwald basement (Table 2; Figs. 4e–g, 5c). The regression of all data points ($n = 78$) yields a well-constrained age of 316 ± 4 Ma for monazite growth in these rocks (Table 2). Distinctly older, Upper Visean ages of 331 ± 28 Ma (Sample EH 6) and 329 ± 19 Ma (Sample KK 7; Fig. 5d) were determined for monazite grains from the eastern Odenwald orthogneiss (Fig. 4i, j). All data

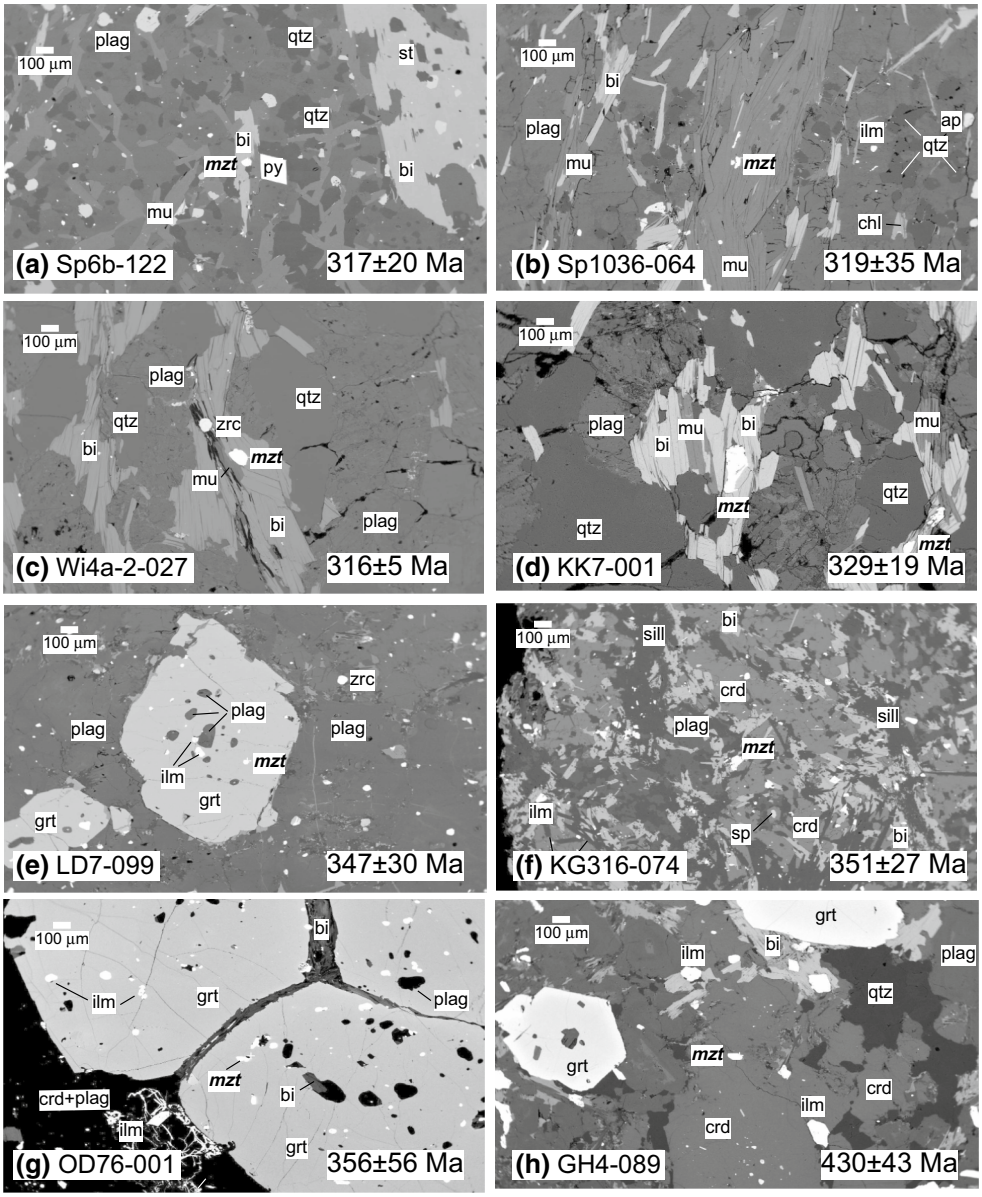

Fig. 5 Backscattered electron images showing the textural position of monazite grains used for in situ electron microprobe dating: **a** sample Sp 6b, **b** sample Sp 1036, **c** sample Wi 4a-2, **d** sample KK7, **e** sample LD7, **f** sample KG316, **g** sample OD76, **h** sample GH4. Samples Sp 6b and Sp 1036 are amphibolite-facies metapelitic schists from the central Spessart basement, and sample Wi 4a-2 is an upper greenschist- to amphibolite-facies metapsammitic rock from the eastern Odenwald basement. Sample KK7 is a metagranodiorite from the eastern Odenwald basement, and the remaining samples are granulite-facies paragneiss samples from the western Odenwald basement. The weighted average monazite crystallisation ages and their 2σ standard deviations are shown. The measured monazite grains are indicated in *bold*, *italicised lettering*. Mineral abbreviations are defined in caption to Table 2; additional abbreviations are: mzt, monazite; ilm, ilmenite; py, pyrite; ap, apatite

points ($n = 31$) provide a monazite age of 331 ± 16 Ma for the orthogneiss samples (Table 2).

Age of monazite growth in the western Odenwald (upper plate)

The same samples that were used by Will and Schmädicke (2003) to constrain the counterclockwise *P–T* path of the western Odenwald granulites were re-used to determine the age of monazite growth in these rocks. Samples LD 3, LD 7, KG 316 and OD 76 from near the township of Laudenau (Fig. 2) provided Upper Tournaisian ages of 345 ± 30 Ma, 347 ± 30 Ma, 351 ± 21 Ma and 356 ± 56 Ma, respectively (Table 2; Figs. 4l–o, 5e–g). Regressing all Laudenau granulite data ($n = 62$) yields an age of 349 ± 14 Ma (Table 2). The high-grade garnet-rich paragneiss GH 4

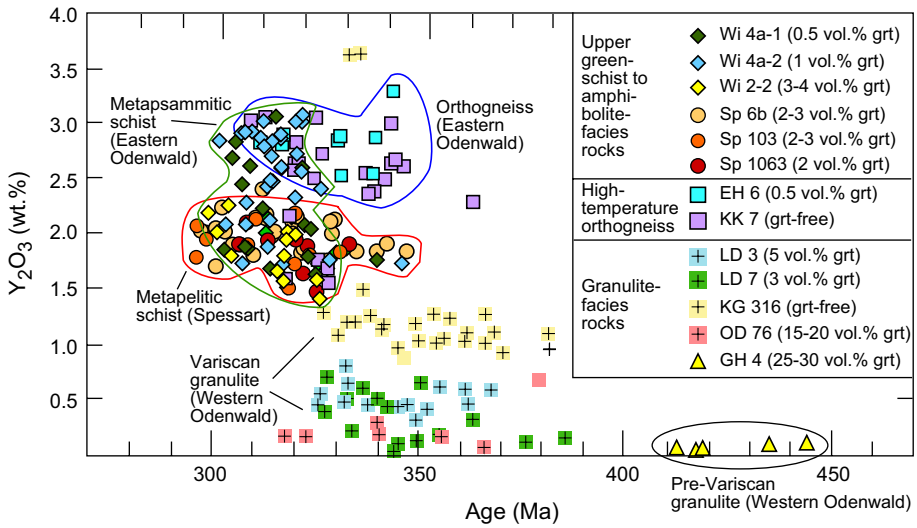

Fig. 6 Variation of monazite Y_2O_3 concentrations with Th–U–Pb apparent model age. Note the extremely low Y_2O_3 contents in the pre-Variscan monazite grains of the granulite from Gadernheim in the western Odenwald (Sample GH4)

from Gadernheim (Fig. 2) differs from the garnet-poor Laudenau granulite because it lacks spinel but contains quartz (Will and Schmädicke 2003) and provided a less well-constrained ($n = 6$), but nevertheless significantly older, pre-Variscan Silurian age of 430 ± 43 Ma (Table 2; Fig. 5h). Variscan monazite ages were not obtained from this sample.

Interpretation

Crystallisation order of monazite and garnet

The mineral chemistry of monazite provides additional constraints on the conditions of its crystallisation. Significant variations in rare earth elements and Y_2O_3 in monazite with varying metamorphic grade and age are known (e.g. Spear and Pyle 2002). For example, experimental studies by Heinrich et al. (1997) showed that Y_2O_3 contents in monazite coexisting with xenotime increase with temperature. Another factor, which influences the content of Y_2O_3 in monazite is the presence or absence of Y_2O_3-fractionating minerals such as garnet. As demonstrated by several authors (e.g. Pyle et al. 2001; Spear and Pyle 2002; Schulz and von Raumer 2011), monazite in garnet-free samples is usually enriched in Y_2O_3 compared to garnet-bearing samples. Figure 6 shows the content of Y_2O_3 in monazite plotted versus apparent age. As obvious from this diagram, there is no positive correlation between Y_2O_3 concentration and metamorphic grade. However, monazite grains in the high-grade granulitic paragneiss of the western Odenwald have significantly lower Y_2O_3 concentrations than monazite grains in the lower-grade garnet-staurolite and garnet-biotite schists of the eastern Odenwald–Spessart basement. In addition, a correlation between the modal amount of garnet and the monazite Y_2O_3 concentration is plausible. Monazite grains in all Spessart samples and the eastern Odenwald sample Wi 2-2 have intermediate to elevated Y_2O_3 contents of 1.5–2.2 wt%, with the modal amount of garnet ranging from 2 to 4 vol%. Samples Wi 4a-1 and Wi 4a-2 contain less garnet (0.5–1 vol%), and even though the Y_2O_3 values overlap partly with those of samples Sp 6b, Sp 103, Sp 1063 and Wi 2-2, they are generally higher and reach up to 3.1 wt% (Fig. 6, Electronic Supplement Table S2). The orthogneiss samples of the eastern Odenwald (EH6 and KK7) have the highest monazite Y_2O_3 contents (2.4–3.3 wt%) of all samples; these rocks are either garnet-free (Sample KK 7) or contain only a trace amount of garnet (Sample EH 6). The granulite-facies metapelitic rocks of the western Odenwald are either garnet-free (Sample KG 316) or contain variable amounts of garnet. The samples that provided Variscan monazite ages show a remarkable correlation between Y_2O_3 concentration in monazite and the modal amount of garnet in the granulites. Sample OD 76 contains c. 15–20 vol% garnet, with generally very low monazite Y_2O_3 values of less than 0.3 wt% (with one exception). Y_2O_3 content in samples LD 3 and LD 7 (5 and 3 vol% garnet, respectively) is generally higher up to 0.9 wt%, and the garnet-free sample KG 316 has the highest Y_2O_3 value of all western Odenwald granulite samples (Fig. 6). The pre-Variscan granulite GH 4 with c. 25–30 vol% garnet provided only a few but very Y_2O_3-poor monazite grains, with Y_2O_3 values of less than 0.09 wt%.

The crystallisation order of garnet and monazite has a profound influence on the Y_2O_3 concentration in monazite because Y_2O_3 is strongly fractionated into garnet (e.g. Pyle et al. 2001). Thus, monazite grains that crystallised prior to garnet are typically enriched in Y_2O_3 compared to monazite that grew after or during garnet growth. This fact provides additional support for the

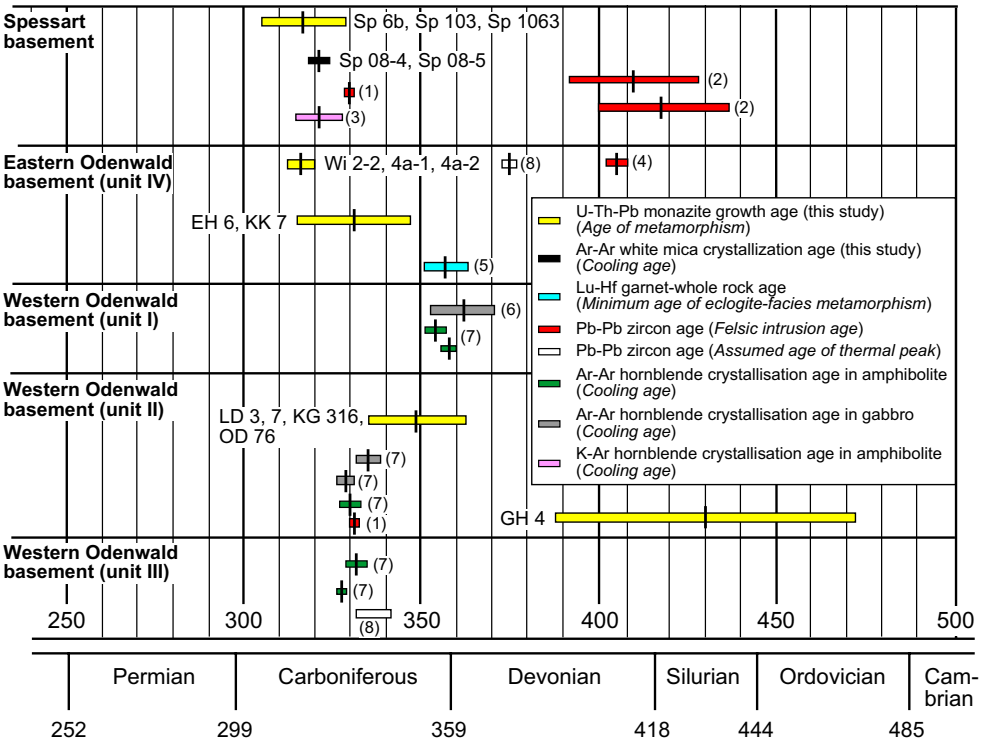

Fig. 7 Time-space diagram for the Odenwald–Spessart basement. System ages according to Cohen et al. (2013; updated 2015). The interpretation of the geochronological data is given in *italics*. A cooling age corresponds to the time at which a mineral cooled through a specific temperature (closure temperature) that is in the order of c. 350 and 500–550 °C for white mica and hornblende, respectively (Hodges 2003). *Source* of geochronological data: *1* Siebel et al. (2012), *2* Dombrowski et al. (1995), *3* Nasir et al. (1991) and Lippolt (1986), *4* Reischmann et al. (2001), *5* Scherer et al. (2002), *6* Kirsch et al. (1988), *7* Schubert et al. (2001), *8* Todt et al. (1995)

pre- or Eo-Variscan monazite age of the western Odenwald high-grade paragneiss GH 4 from Gadernheim. This sample is very much garnet-rich (see above) and contains Silurian-age monazite grains with very low Y_2O_3 concentrations of less than 0.09 wt% (Electronic Supplement Table S2). A possible magmatic or detrital origin of the monazite grains is ruled out because of their lack of magmatic zoning, chemistry and the similar apparent ages of the individual grains (Electronic Supplement Table S2). Hence, crystallisation of the 430 ± 43-Ma-old monazite grains must overlap with, or even post-date the high-temperature garnet growth in sample GH4. Thus, garnet growth and the granulite-facies metamorphism recorded by this sample cannot be younger than Silurian. The same logic can be applied to the interpretation of other samples with low- and intermediate-Y_2O_3 monazite grains. In the garnet-bearing samples LD 3, LD 7 and OD 76, the low monazite Y_2O_3 concentrations indicate that the Upper Tournaisian monazite growth age of 349 ± 14 Ma provides a minimum age for granulite-facies metamorphism as it post-dates garnet growth at the thermal peak, even if only slightly. The garnet-staurolite and garnet-biotite schists of the eastern Odenwald–Spessart basement have similar modal amounts of garnet and intermediate to elevated Y_2O_3 concentrations in monazite. The determined ages of 317 ± 12 Ma and 316 ± 4 Ma are therefore interpreted to date monazite growth slightly before or at the amphibolite-facies metamorphic peak. Our new geochronological data, together with available petrological and

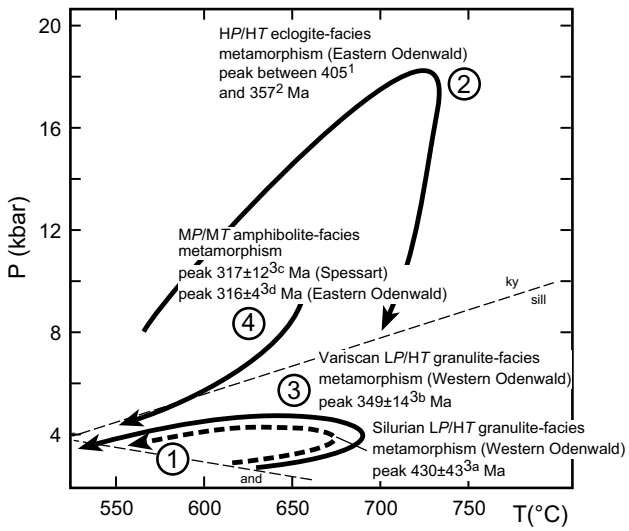

Fig. 8 Summary of pressure–temperature–time (*P–T–t*) diagram for various lithologies of the Odenwald–Spessart basement. The *P–T* paths are modified after Will and Schmädicke (2001, 2003) and Will (1998). *Source* of age data: *1* Reischmann et al. (2001), *2* Scherer et al. (2002), *3* this study: *3a* granulite (Gadernheim, western Odenwald), *3b* granulite (Laudenau, western Odenwald), *3c* Garnet-staurolite schist (central Spessart), *3d* Garnet-bearing metapsammitic schist (eastern Odenwald). The aluminium silicate stability fields are shown for reference (ky, kyanite; sill, sillimanite; and, andalusite)

geochronological data, are summarised in Figs. 7 and 8 and are used for the interpretation of the geologic history of the Odenwald–Spessart basement.

Eastern Odenwald–Spessart basement

The orthogneiss precursor rocks of the eastern Odenwald–Spessart basement are interpreted to be of volcanic arc origin (Altenberger and Besch 1993; Dombrowski et al. 1995) and intruded at c. 418–410 ± 18 Ma in the central Spessart (Dombrowski et al. 1995) and between 410 and 405 Ma in the eastern Odenwald (Reischmann et al. 2001). Several authors (e.g. Linnemann et al. 2007; Zeh and Will 2010; Eckelmann et al. 2014) proposed that the intrusions took place in a Upper Silurian to Lower Devonian magmatic arc setting at the northern margin of the Rheic Ocean. The eastern Odenwald orthogneiss contains relics of high-pressure eclogite that provided a minimum age of metamorphism of 357 ± 6 Ma (Scherer et al. 2002). Thus, arc accretion must have occurred prior to 357 Ma and subduction of the (presumed) Rheic Ocean must already have been underway at that time. The remarkable similarity of our new $^{40}Ar/^{39}Ar$ and EMP monazite ages (Fig. 7) that are indistinguishable to results presented by Nasir et al. (1991) and Dombrowski et al. (1995) is taken as evidence that the Barrow-type metamorphism in the eastern Odenwald–Spessart tectonic window, reaching peak conditions of c. 630–650 °C at ~8 kbar in the Spessart basement (Fig. 8), took place between c. 324 and 318 Ma. This also corresponds to the time of metamorphic monazite growth in the eastern Odenwald basement schist unit at c. 316 Ma (Fig. 7). As a corollary, the Variscan collision and deformation associated with crustal thickening and closure of the Rheic Ocean must have been underway at that time. In addition, the eastern Odenwald orthogneiss unit yielded a weighted monazite age of 331 ± 16 Ma, which, within uncertainty, overlaps with the monazite ages of the eastern Odenwald–Spessart basement schists.

Western Odenwald basement

Our new monazite data for the granulite sample GH4 from Gadernheim provide evidence for a pre- or Eo-Variscan high-temperature event at c. 430 ± 43 Ma (Figs. 4, 7). Detailed petrological investigations of this rock showed that the granulite underwent a counterclockwise *P–T* path with maximum pressures not exceeding 4–5 kbar at temperatures well above 650 °C (Will and Schmädicke 2003; Fig. 8). These peak metamorphic conditions are very favourable for monazite crystallisation (Spear 2010) and are also typical for a magmatic arc setting. Associated arc rocks of that age are not yet known from the western Odenwald basement but are present in the eastern Odenwald–Spessart basement (see above) and are also described from localities to the west of the exposed Odenwald basement area. Calc-alkaline granitoid rocks recovered from the Borehole Saar 1 (Fig. 1) provided a Pb–Pb zircon age of 444 ± 22 Ma, which was interpreted as the time of intrusion (Sommermann 1993). In addition, 433 ± 3-Ma-old zircon grains were dated in a calc-alkaline granitic gneiss from the Palatinate (Reischmann and Anthes 1996) and a quartz phyllite from the Taunus area yielded a white mica $^{40}Ar/^{39}Ar$ crystallisation age of 437 ± 5 Ma (pers. comm. L. Ratschbacher and J. Pfänder, unpubl. data). The timing of the c. 430 ± 43-Ma metamorphic event of the Gadernheim granulite is not very precise but overlaps with the Silurian intrusion ages of the calc-alkaline magmatic rocks referred to above. Despite its present-day occurrence, the Gadernheim granulite is most likely allochthonous to the western Odenwald as Silurian to Lower Devonian calc-alkaline rocks are not known from this area. In addition, the Gadernheim granulite is petrologically distinct from other western Odenwald high-grade rocks as it is quartz-bearing and very garnet-rich (Will and Schmädicke 2003).

Samples from the Laudenau area, only a few kilometres to the east of Gadernheim (Fig. 2), provide indisputable evidence for a second high-temperature event in the western Odenwald. Will and Schmädicke (2003) showed that the Laudenau granulite, like the Gadernheim samples, experienced a counterclockwise, hairpin-like *P–T* path with peak pressures of 4–5 kbar and temperatures well in excess of 640 °C (Fig. 8), being typical of a magmatic arc setting. The same granulite-facies samples investigated by Will and Schmädicke (2003) were re-used for monazite age dating and provided a Lower Carboniferous minimum age of 349 ± 14 Ma for monazite growth and high-grade metamorphism. A Lower Carboniferous arc setting appears also to be compatible with the presence of mantle-derived calc-alkaline gabbroic rocks that intruded the western Odenwald at c. 360 Ma (Kirsch et al. 1988; Schubert et al. 2001) and ubiquitous calc-alkaline dioritic to granitic bodies that intruded the area between c. 340 and 330 Ma (Kreuzer and Harre 1975; Siebel et al. 2012).

Pressure–temperature–time history of metamorphism in the Odenwald–Spessart basement

The new geochronological data presented in this study and the available petrological constraints are summarised in Fig. 8. The counterclockwise *P–T* paths document the tectonothermal history of the pre-Variscan (path 1, stippled) and Variscan (path 3) high-grade granulites in the western Odenwald, with metamorphic peak conditions being reached at c. 430 and 350 Ma, respectively. Path 2 shows the clockwise trajectory of the eastern Odenwald eclogite; the metamorphic peak occurred prior to 357 Ma. The metapelitic rocks from the eastern Odenwald–Spessart basement were metamorphosed up to amphibolite-facies conditions at c. 320 Ma. The *P–T* path of these rocks is represented by trajectory 4.

Discussion and regional geological implications

Will et al. (2015) proposed that the Otzberg–Michelbach Fault Zone (Fig. 1) marks the boundary between Gondwana- and Baltica/Avalonia-derived terranes in the Odenwald–Spessart basement. This idea strengthens earlier ideas (e.g. Krohe 1992, 1996; Oncken 1997; Will 2001) and is in analogy to, and consistent with, findings presented by Zeh and Gerdes (2010) who argued that the Ruhla basement (Fig. 1), some 150 km NE of the Odenwald–Spessart basement, consists of two crustal terranes with distinct Gondwana and Avalonia heritage. Accepting the terrane concept as valid implies that the eastern Odenwald–Spessart basement forms a tectonic window of lower plate Baltica/Avalonia-derived rocks within the upper plate Gondwana-related terrane that constitutes the western Odenwald and the northernmost part of the Spessart basement (Alzenau Formation). In this context, the Otzberg–Michelbach Fault Zone defines the western outcrop limit of the Spessart–eastern Odenwald tectonic window (Will et al. 2015). Allochthonous slivers of lower plate rocks such as the pre-Variscan, 430 ± 43-Ma-old Silurian Gadernheim granulite are locally exposed within upper plate, Gondwana-derived metasedimentary rocks.

The Baltica and Avalonia connection: a pre-Variscan magmatic arc

The protoliths of the metasedimentary rock, orthogneiss and most amphibolite in the central Spessart basement formed in a continental volcanic arc setting (Dombrowski et al. 1995; Will et al. 2015), possibly at the active Avalonian margin of the Rheic Ocean (e.g. Linnemann et al. 2007; Zeh and Will 2010; Eckelmann et al. 2014). Intrusion of the calc-alkaline orthogneiss precursor rocks into the sedimentary sequence took place in the Upper Silurian to Lower Devonian (Dombrowski et al. 1995; Reischmann et al. 2001). Thus, a pre-Upper Silurian deposition age is indicated for the metasedimentary precursor rocks of the Spessart–eastern Odenwald tectonic window and, by implication, for the Gadernheim granulite (see above), and the protoliths of these basement rocks are interpreted to have formed in a volcanic arc setting at the northern margin of the Rheic Ocean prior to the Lower Devonian. Zeh and Will (2010) proposed that this pre-Variscan arc magmatism formed in response to NW-directed subduction of the Rheic Ocean underneath the Avalonian margin, with recycling of older crustal material having been an important process during the Upper Silurian to Lower Devonian arc magmatism (Will et al. 2015).

Several authors (e.g. von Raumer and Stampfli 2008; Zeh and Gerdes 2010; Stampfli et al. 2013) suggested that the subduction direction of the Rheic Ocean changed from NW to SE in the Devonian. This may have been caused by the formation of a short-lived Rhenohercynian back-arc basin (e.g. Oncken et al. 2000; Eckelmann et al., 2014), which split the Avalonian margin into a northern and a southern segment. If true, this change in subduction polarity resulted in tectonic quiescence at the formerly active pre-Variscan arc at the Avalonian margin of the Rheic Ocean. Instead, tectonic activity would have shifted south and a Variscan arc emerged at the Gondwana margin of the Rheic Ocean (Gerdes and Zeh 2006; Zeh and Will 2010) or within the Rheic Ocean (Eckelmann et al. 2014).

The Gondwana connection: a Variscan magmatic arc

The protoliths of the metasedimentary rocks of inferred Gondwana origin in the western Odenwald and other areas of the Mid-German Crystalline Zone (Fig. 9) were deposited at the northwestern margin of Gondwana after the Upper Cambrian/Lower Ordovician (e.g. Gerdes and Zeh 2006; Linnemann et al. 2007). Evidence of Silurian to Devonian igneous activity has not yet been recognised in the Gondwana-derived basement areas of the Mid-German Crystalline Zone (Zeh and Will 2010).

As a result of the proposed change of the subduction direction of the Rheic Ocean, a Variscan magmatic arc developed at the northern margin of Gondwana. At 362 ± 9 Ma (Kirsch et al. 1988), mantle-derived gabbroic rocks exposed in unit I of the western Odenwald basement were emplaced into this setting and coeval amphibolite-facies metamorphism occurred at 360 ± 2 to 354 ± 3 Ma (Schubert et al. 2001). Our new monazite data constrain the arc-related metamorphic event in the western Odenwald to 349 ± 14 Ma, which overlaps with, or slightly predates, intrusions of calc-alkaline dioritic to granitic bodies at c. 340–330 Ma (e.g. Kreuzer and Harre 1975; Siebel et al. 2012) and also coincides with the timing of other granulite-facies events in many areas of the central European Variscides (e.g. Kroner and Romer 2013). In addition, amphibolite-facies metabasic rocks of inferred back-arc origin (e.g. Poller et al. 2001; Will et al. 2015) provided (cooling) ages of c. 332–328 Ma (Schubert et al. 2001).

J. von Raumer (pers. comm. 2016) suggested that the 349 ± 14-Ma-old granulite-facies metamorphism in the western Odenwald could be related to contact metamorphism. This, of course, is possible but many intrusive rocks in the western Odenwald are arc-related rocks that are interpreted to have formed in a supra-subduction setting (e.g. Altherr et al. 1999; Poller et al. 2001; Will et al. 2015). As granulite-facies conditions are typical for a subduction zone setting, we interpret the high-temperature episode at c. 350 Ma as a subduction-related event, which could have been accompanied by (regional) contact metamorphism as already speculated upon by Will and Schmädicke (2001).

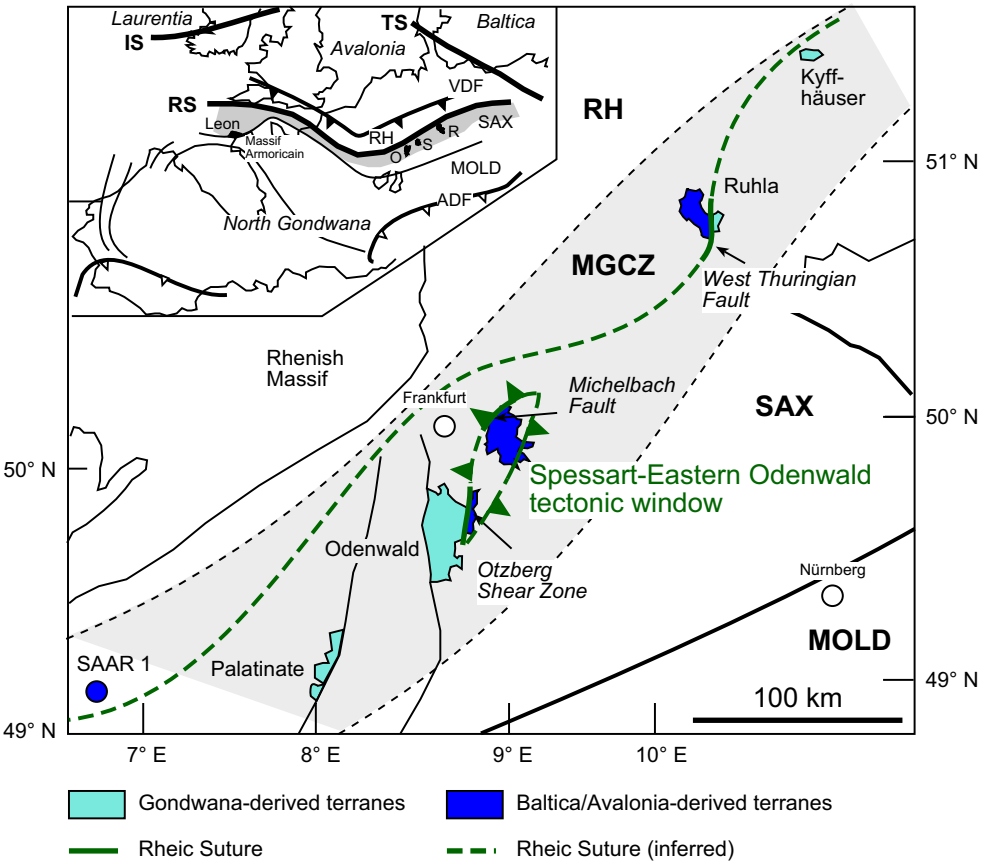

Fig. 9 Inferred location of the Rheic Suture within the Mid-German Crystalline Zone (*shaded in grey* only the exposed areas are shown on the map), modified after Will et al. (2015). The eastern Odenwald and the Spessart (except for its northernmost part) are interpreted as Baltica/Avalonia-derived units exposed in a tectonic window beneath the suture. The Baltica/Avalonia-derived crustal terrane comprises Silurian to Devonian magmatic arc and medium- to high-pressure metamorphic rocks, whereas the Gondwana-derived terrane includes Variscan magmatic arc and high-grade metamorphic rocks. Juxtaposition of the Baltica/Avalonia- and Gondwana-derived crustal terrane occurred between 324 and 318 Ma. For abbreviations see caption to Fig. 1

Nevertheless, of prime importance for unravelling the geologic history of the area is the existence of a subduction zone and the associated convergence between Gondwana and Baltica/Avalonia in the Lower Carboniferous.

Assembly of the Mid-German Crystalline Zone

Collision between Baltica/Avalonia and the peri-Gondwana arc was accompanied by initial N- to NW-directed thrusting, which is consistent with the Carboniferous SE-directed subduction of the Rheic Ocean. This changed to transpressive, sinistral shearing and strike-slip tectonics (e.g. Krohe 1992, 1996; Oncken 1997; Will 2001; Stephan et al. 2016) and caused, or was associated with, Barrow-type amphibolite-facies metamorphism in the eastern Odenwald–Spessart basement (Will 1998; Marx 2008) and parts of the Ruhla basement further to the northeast (Zeh 1996). These medium-pressure conditions are typical for collisional tectonics and associated crustal thickening during plate convergence. Our new monazite data constrain this event to 317 ± 12 Ma in the Spessart basement and to 316 ± 4 Ma in the eastern Odenwald basement. The $^{40}Ar/^{39}Ar$ ages of 322 ± 3 and 324 ± 3 Ma for white mica crystallisation in central Spessart mica schist are in agreement with the monazite data and further strengthen the recent proposition of a common geological evolution of the eastern Odenwald–Spessart basement (Will et al. 2015). Additionally, the similarity of the monazite growth and the white mica $^{40}Ar/^{39}Ar$ cooling ages are consistent with the notion of rapid exhumation of the metamorphic pile. The cause of exhumation is currently unknown but might be related to the existence of an extrusion wedge during lithospheric convergence.

Diachronous, oblique juxtaposition of the Gondwana- and Baltica/Avalonia-derived terranes must have occurred in the Upper Carboniferous along the Otzberg–Michelbach Fault Zone (Will 2001). Based on our new age data, this should have occurred shortly after the peak of the Barrow-type metamorphism in the eastern Odenwald–Spessart basement between c. 324 and 318 Ma (see above). The inferred position of the resulting Rheic Suture, the location of the Spessart–eastern Odenwald tectonic window and the spatial distribution of the two main tectonic units are shown in Fig. 9. Both the Mid-German Crystalline Zone and the Rheic Suture are likely to continue into the Léon Domain in the northern part of the French Massif Armoricain and further south into the Iberian Massif, where geochronological, geochemical and petrological data of lithologies very similar to those exposed in the Odenwald and Spessart basement indicate a similar geological evolution (e.g. Ballèvre et al. 2009; Faure et al. 2010; Schulz 2013; von

Raumer et al. 2015; Villaseca et al. 2015). To the east, the c. 385–380-Ma-old Ślęża ophiolite in the central Sudetes is interpreted to trace the Rheic Suture in Lower Silesia, SW Poland (Kryza and Pin 2010; Nance et al. 2012).

Conclusion

From available petrological, geochronological and our new monazite and $^{40}Ar/^{39}Ar$ data (Fig. 7), the following conclusions are drawn:

1. Th–U–Pb in situ monazite age dating of metasedimentary rocks and orthogneiss samples from the Odenwald–Spessart basement provides evidence for distinct thermal events at c. 430, 349, 331 Ma and 317–316 Ma (Figs. 4, 7; Tables 1, 2). Granulite from Gadernheim in the western Odenwald experienced a counterclockwise *P–T* path and reached peak temperatures at c. 430 ± 43 Ma. These rocks do not contain evidence for previous or subsequent thermal events. At 349 ± 14 Ma, a further high-temperature event is recorded in the western Odenwald basement, which caused granulite-facies metamorphism of metapelitic rocks now exposed near Laudenau. Indications of older or younger thermal event are not preserved in these samples. Like the c. 80-myr-old samples from Gadernheim, the Laudenau granulite underwent a counterclockwise metamorphic evolution. Amphibolite-facies metamorphism occurred coevally in the eastern Odenwald schist unit at 316 ± 4 Ma and in the central Spessart basement schists at 317 ± 12 Ma. These ages overlap and are consistent with white mica $^{40}Ar/^{39}Ar$ ages of 322 ± 3 Ma and 324 ± 3 Ma for mica schist from the central Spessart basement, possibly indicating rapid exhumation and cooling.
2. The Odenwald–Spessart basement and the Mid-German Crystalline Zone consist of at least two distinct crustal terranes of different origins that experienced contrasting geological histories prior to their juxtaposition in Upper Variscan times. Based on the available geological record, the Spessart and eastern Odenwald basement rocks and, in addition, those of the NW segment of the Ruhla basement (Zeh and Gerdes 2010) are inferred to be derived from a Baltica/Avalonia source and/or formed at the active Avalonian margin of the Rheic Ocean. The Silurian high-temperature granulite near Gadernheim appears to be allochthonous to the western Odenwald and is most likely a displaced splinter of the eastern Odenwald–Spessart basement. In contrast, the Carboniferous high-temperature granulite in the western Odenwald originated at the northern Gondwana margin.
3. Our new age data strengthen the proposition by Will et al. (2015) that the combined Otzberg–Michelbach Fault Zone constitutes the boundary between two distinct crustal terranes of different geological heritage in the Odenwald–Spessart basement. Thus, it is considered as a major Variscan terrane boundary between Gondwana- and Avalonia-derived terranes in the Odenwald–Spessart basement and, by implication, in the entire Mid-German Crystalline Zone.
4. Based on the contrasting pressure–temperature paths of the eastern and western Odenwald basement domains (Fig. 8), Will and Schmädicke (2003) interpreted the Odenwald as a paired metamorphic belt. The Carboniferous high-temperature metamorphism in the western Odenwald was constrained at 349 ± 14 Ma, which overlaps with the minimum estimate for high-pressure metamorphism in the eastern Odenwald at 357 ± 6 Ma (Scherer et al. 2002). Admittedly, the high-pressure event could be older but without more precise information on the timing of the eclogite-facies metamorphism, and given the overlapping ages of granulite- and eclogite-facies metamorphism, we follow the original interpretation of Will and Schmädicke (2003) and consider the Odenwald as a paired metamorphic belt. Moreover, it should be kept in mind that the time of peak metamorphism may differ across the area because granulite- and eclogite-facies conditions were reached at different depths at different times. Thus, we argue that the high-pressure and high-temperature rocks were metamorphosed in the same subduction zone system during the Lower Carboniferous and were subsequently juxtaposed along the Rheic Suture during the final assembly of the central European Variscan orogen.

Acknowledgments P. Späthe (Würzburg) is thanked for the superb thin section preparation and V. von Seckendorff (formerly at Erlangen; now Würzburg) for his assistance with the monazite analysis. L. Ratschbacher, J. Pfänder and co-workers of the Argonlab at the TU Bergakademie Freiberg, Germany, are thanked for the $^{40}Ar/^{39}Ar$ analyses and age determinations. W. Dörr and J. von Raumer provided fair and helpful reviews. In addition, J. von Raumer is sincerely thanked for his continued interest in this work and for his many suggestions regarding the origin of the Odenwald rocks.

Appendix 1: $^{40}Ar/^{39}Ar$ dating

We performed $^{40}Ar/^{39}Ar$ dating at the Argonlab of the TU Bergakademie Freiberg, Germany (Pfänder et al. 2014). The micas were handpicked and ultrasonically cleaned in acetone and deionised water. After drying, they were wrapped into Al foil and loaded in 5 × 5 mm wells on 33-mm Al discs stacked together for irradiation. Cadmium-shielded neutron irradiation of samples and fluence monitors was done for 7 h in the RODEO facility of the HFR research reactor in Petten, The Netherlands. The irradiated micas were unwrapped,

and 2.5–3.0 mg aliquots were loaded in 3 × 1 mm (diameter × depth) wells on an oxygen-free copper disc and transferred to the sample chamber. We performed step heating using a floating 10.6 µm CO_2 laser system with a defocused beam at 3 mm diameter, followed by gas purification applying two AP10 N getter pumps, one at room temperature and one at 400 °C. Heating time was 5 min; cleaning time was 10 min per step. Ar isotope compositions of individual temperature steps were measured in static mode using an ARGUS noble gas mass spectrometer equipped with five faraday cups and 10^{12} Ohm resistors on mass positions 36–39 and a 10^{11} Ohm resistor on mass position 40. Typical blank levels were 2.5×10^{-16} mol^{40}Ar and 8.1×10^{-18} mol^{36}Ar. Measurement time was 7.5 min per step acquiring 45 scans at 10-s integration time each. Mass bias was corrected assuming linear mass-dependent fractionation and using an atmospheric $^{40}Ar/^{36}Ar$ ratio of 295.5. Raw data reduction employed an in-house developed Matlab® toolbox; inverse isochron and plateau ages were calculated using Isoplot 3.7 (Ludwig 2008). Ages were calculated against Fish Canyon Tuff sanidine (FCT) as flux monitor (28.305 ± 0.036 Ma; Renne et al. 2010). Corrections for interfering Ar isotopes were done using the ratios as given in Electronic Supplement Table S1 and applying 5 % uncertainty. Repeatedly measured HDB1 biotite, irradiated in several batches along with FCT and unknowns, yielded an average age of 24.68 Ma at an external reproducibility better 0.9 % (1σ, $n = 5$). Complete step heating data and intensity intercept values are presented in the Electronic Supplement Table S1.

Appendix 2: Th–U–Pb electron microprobe (EMP) monazite dating

The electron microprobe (EMP) Th–U–Pb dating is based on the observation that common Pb concentration in monazite (LREE, Th)PO_4 is negligible with respect to radiogenic Pb contents that result from the decay of Th and U (e.g. Suzuki et al. 1994; Montel et al. 1996). As Th concentrations in magmatic and metamorphic monazite are generally high, a sufficient amount of radiogenic Pb that is measureable by the EMP analysis accumulates in monazite within >100 myr (Schulz and Schüssler 2013). Thus, EMP analyses of bulk Th, U and Pb concentrations in monazite can be used for the calculation of a chemical model age and the associated error (e.g. Montel et al. 1996; Cocherie and Albarède 2001; Suzuki and Kato 2008; Spear et al. 2009).

Analyses of ThO_2, UO_2, PbO, light rare earth elements (LREE), Y_2O_5, CaO, SiO_2 and P_2O_5 concentrations in monazite grains (Electronic Supplement Table S2) were used to calculate monazite chemical ages following two different approaches. First, following the approach outlined by Montel et al. (1996), an age was calculated for each individual analysis, with the 1σ standard deviation resulting from counting statistics being in the order of c. 20–40 myr for the Palaeozoic samples (Electronic Supplement Table S2). Using these apparent age data, weighted average ages and related errors for monazite populations in the samples were then calculated using Isoplot 3.7 (Ludwig 2008) and are interpreted as the age of monazite growth or recrystallisation during metamorphism (Table 2 and Electronic Supplement Table S2). Second, ages were also determined using the ThO_2^*-PbO isochron method (the chemical isochron method 'CHIME' of Suzuki et al. 1994), where ThO_2^* is the sum of the measured ThO_2 plus ThO_2 equivalent to the measured UO_2. The age is proportional to the slope of a regression line that is forced through zero in ThO_2^* versus PbO space. The model ages obtained by the two different methods coincide exceptionally well in all samples analysed (Electronic Supplement Table S2, Fig. 4).

Th, U and Pb concentrations in monazite grains were determined for the calculation of monazite model ages, and Ca, Si, P, LREE and Y contents were measured for corrections and determination of the monazite mineral chemistry. All in situ thin section analyses were carried out with a JEOL JXA 8200 at the GeoZentrum Nordbayern, University of Erlangen-Nürnberg, Germany. The Mα1 lines of Th and Pb and the Mβ1 lines of U on a PETH crystal were selected for monazite analysis. Analytical errors of 2σ at 20 kV acceleration voltage, 100-nA beam current, 5-µm-beam diameter and counting times of 320 s (Pb Mα1), 80 s (U Mβ1) and 40 s (Th Mα1) on peak have been used for age calculations. The error on Pb concentrations typically ranges from 0.016 to 0.024 wt%. Synthetic orthophosphates from the Smithsonian Institution were used as standards for the REE analysis (Jarosewich and Boatner 1991). The Lα1 lines were chosen for the analysis of La, Y and Ce and the Lβ1 lines for Pr, Sm, Nd and Gd. The Si, P and Ca concentrations were analysed on the Kα1 lines. Calibration of PbO was carried out on a vanadinite standard. The U was calibrated on a glass standard with 5 wt% UO_2. Following the procedure outlined by Schulz and Schüssler (2013), monazite from a pegmatite in Madagascar (*Madmon*) was used for the calibration of ThO_2 and as a reference for the EMP analyses. The analytical results of the standard measurements are given in Electronic Supplement Table S3. As summarised by Schulz and Schüssler (2013), the age of the *Madmon* reference standard is well known and was determined by different techniques providing ages of 496 ± 9 Ma (concordant SHRIMP U–Pb age), 497 ± 2 Ma (TIMS Pb–Pb evaporation age) and 502 ± 6 Ma and 503 ± 6 Ma, respectively (EMP chemical model ages). The minor Y interference on the Pb Mα1 line was corrected by linear extrapolation after measuring several Pb-free yttrium glass standards with 5 and 12 wt% Y_2O_3 (Montel et al. 1996). The interference of Th Mγ on U Mβ was also empirically corrected, and a Gd interference on

U Mβ requires correction if Gd_2O_3 in monazite is larger than 5 wt%. These parameters and measurement conditions were chosen to counter the analytical problems and limits of the method as discussed by various authors (e.g. Williams et al. 2006; Jercinovic et al. 2008; Suzuki and Kato 2008; Spear et al. 2009).

References

Altenberger U, Besch T (1993) The Böllstein Odenwald: evidence for pre- to early-Variscan plate convergence in the Central European Variscides. Geol Rundsch 82:475–488

Altherr R, Henes-Klaiber U, Hegner E, Satir M (1999) Plutonism in the Variscan Odenwald (Germany): from subduction to collision. Int J Earth Sci 88:422–443

Anthes G, Reischmann T (2001) Timing of granitoid magmatism in the eastern Mid-German Crystalline Rise. J Geodyn 31:119–143

Ballèvre M, Bosse V, Ducassou C, Pitra P (2009) Palaeozoic history of the Armorican Massif: models for the tectonic evolution of the suture zones. C R Geosci 341:174–201

Behr HJ, Heinrichs T (1987) Geological interpretation of DEKORP 2-S: a deep seismic reflection profile across the Saxothuringian and possible implications for the late Variscan structural evolution of Central Europe. Tectonophysics 142:173–202

Chatterjee ND (1960) Geologische Untersuchungen im Kristallin des Böllsteiner Odenwaldes. N Jb Geol Paläontol Abh 37:223–256

Cherniak DJ, Watson EB, Grove M, Harrison TM (2002) Pb diffusion in monazite. Geol Soc Am Abstr Prog 34(6)

Cocherie A, Albarède F (2001) An improved U–Th–Pb age calculation for electron microprobe dating of monazite. Geochim Cosmochim Acta 24:4509–4522

Cohen KM, Finney SC, Gibbard PL, Fan J-X (2013; updated 2015) The ICS international chronostratigraphic chart. Episodes 36:199–204

do Couto D, Faure M, Augier R, Cocherie A, Rossi P, Li XH, Lin W (2016) Monazite U–Th–Pb EPMA and zircon U–Pb SIMS chronological constraints on the tectonic, metamorphic, and thermal events in the inner part of the Variscan orogen, example from the Sioule series, French Massif Central. Int J Earth Sci 105:557–579

Dombrowski A, Henjes-Kunst F, Höhndorf A, Kröner A, Okrusch M, Richter P (1995) Orthogneisses in the Spessart Crystalline Complex, Northwest Bavaria: witnesses of Silurian granitoid magmatism at an active continental margin. Geol Rundsch 84:399–411

Eckelmann K, Nesbor H-D, Königshof P, Linnemann U, Hofmann M, Lange JM, Sagawe A (2014) Plate interactions of Laurussia and Gondwana during the formation of Pangaea—Constraints from U–Pb LA–SF–ICP–MS detrital zircon ages of Devonian and Early Carboniferous siliciclastics of the Rhenohercynian zone, Central European Variscides. Gondwana Res 25:1484–1500

Faure M, Sommers C, Melleton J, Cocherie A, Lautout O (2010) The Léon domain (French Massif Armoricain): a westward extension of the Mid-German Crystalline Rise? Structural and geochronological insights. Int J Earth Sci 99:65–81

Gerdes A, Zeh A (2006) Combined U–Pb and Hf isotope LA–(MC)–ICP–MS analyses of detrital zircons: comparison with SHRIMP and new constraints for the provenance and age of an Armorican metasediment in Central Germany. Earth Planet Sci Lett 249:47–61

Heinrich W, Andrehs G, Franz G (1997) Monazite-xenotime miscibility gap thermometry. I. An empirical calibration. J Metamorph Geol 15:3–16

Hodges KV (2003) Geochronology and thermochronology in orogenic systems. In: Rudnick RL (ed) The crust. Treatise Geochem 3:263–292

Jarosewich E, Boatner LA (1991) Rare-earth element reference samples for electron microprobe analysis. Geostand Newslett 15:397–399

Jercinovic MJ, Williams ML, Lane ED (2008) In-situ trace element analysis of monazite and other fine-grained accessory minerals by EMPA. Chem Geol 254:197–215

Kirsch H, Kober B, Lippolt HJ (1988) Age of intrusion and rapid cooling of the Frankenstein gabbro (Odenwald, SW Germany) evidenced by $^{40}Ar/^{39}Ar$ and single zircon $^{207}Pb/^{206}Pb$ measurements. Geol Rundsch 77:693–711

Knauer E, Okrusch M, Richter P, Schmidt K, Schubert W (1974) Die metamorphe Basit-Ultrabasit-Assoziation in der Böllsteiner Gneiskuppel, Odenwald. N Jb Mineral Abh 122:186–228

Kreuzer H, Harre W (1975) K/Ar Altersbestimmungen an Hornblenden und Biotiten des Kristallinen Odenwalds. Aufschluss 27:71–77

Krohe A (1992) Structural evolution of intermediate-crustal rocks in a strike-slip and extensional setting (Variscan Odenwald, SW Germany): differential upward transport of metamorphic complexes and changing deformation mechanisms. Tectonophysics 205:357–386

Krohe A (1996) Variscan tectonics of central Europe: postaccretionary intraplate deformation of weak continental lithosphere. Tectonics 15:1364–1388

Kroner U, Romer R (2013) Two plates—many subduction zones: the Variscan orogeny reconsidered. Gondwana Res 24:298–329

Kryza R, Pin C (2010) The Central-Sudetic ophiolites (SW Poland): petrogenetic issues, geochronology and palaeotectonic implications. Gondwana Res 17:292–305

Linnemann U, Gerdes A, Drost K, Buschmann B (2007) The continuum between Cadomian orogenesis and opening of the Rheic Ocean: constraints from LA-ICP-MS U–Pb zircon dating and the analysis of plate-tectonic setting (Saxo-Thuringian zone, NE Bohemian Massif, Germany). In: Linnemann U, Nance RD, Kraft P, Zulauf G (eds) The evolution of the Rheic Ocean: from Avalonian–Cadomian active margin to Alleghenian–Variscan collision. Geol Soc Am Spec Paper 423:61–96

Lippolt HJ (1986) Nachweis altpaläozoischer Primäralter (Rb–Sr) and karbonischer Abkühlalter (K–Ar) der Muscovit–Biotit-Gneise des Spessarts und der Biotit-Gneise des Böllsteiner Odenwaldes. Geol Rundsch 75:569–583

Ludwig KR (2008) User manual for Isoplot 3.70. A geochronological toolkit for microsoft excel. Berkeley Geochron Center Spec Publ 4:1–76

Marx I (2008) Metamorphose-Entwicklung des Spessart-Kristallins, mitteleuropäische Variszide: Phasenpetrologische, mineralchemische und geochemische Untersuchungen an Metapeliten. Unpubl Dissertation, Universität Würzburg

Montel J-M, Foret S, Veschambre M, Nicollet C, Provost A (1996) A fast, reliable, inexpensive in situ dating technique: electron microprobe ages on monazite. Chem Geol 131:37–53

Nance RD, Gutiérrez-Alonso G, Keppie JD, Linnemann U, Murphy JB, Quesada C, Strachan RA, Woodcock NH (2012) A brief history of the Rheic Ocean. Geosci Front 3:125–135

Nasir S, Okrusch M, Kreuzer H, Lenz H, Höhndorf A (1991) Geochronology of the Spessart crystalline complex, Mid-German Crystalline Rise. Mineral Petrol 44:39–55

Nickel E (1975) Geologische Position und Petrogenese des kristallinen Odenwaldes. Aufschluss 27:1–25

Okrusch M, Schubert W, Stähle V (2000) The Odenwald, Germany: Variscan metamorphic evolution and igneous events. Beiheft Eur J Mineral 12:45–89

Oncken O (1997) Transformation of a magmatic arc and an orogenic root during oblique collision and its consequences for the evolution of the European Variscides (Mid-German Crystalline Rise). Geol Rundsch 86:2–20

Oncken O, Plesch A, Weber J, Ricken W, Schrader S (2000) Passive margin detachment during arc-continent collision (Central European Variscides). In: Franke W, Haak V, Oncken O, Tanner D (eds) Orogenic processes: quantification and modelling in the Variscan Belt. Geol Soc Lond Spec Publ 179:199–216

Pfänder JA, Sperner B, Ratschbacher L, Fischer A, Meyer M, Leistner M, Schaeben H (2014) High-resolution 40Ar/39Ar dating using a mechanical sample transfer system combined with a high-temperature cell for step heating experiments and a multicollector ARGUS noble gas mass spectrometer. Geochem Geophys Geosyst 15:2713–2726

Poller U, Altenberger U, Schubert W (2001) Geochemical investigations of the Bergsträsser Odenwald amphibolites—implications for back-arc magmatism. Mineral Petrol 72:63–76

Pyle JM, Spear FS, Rudnick RL, McDonough WF (2001) Monazite-xenotime-garnet equilibrium in metapelites and a new monazite-garnet thermometer. J Petrol 42:2083–2107

Reischmann T, Anthes G (1996) Geochronology of the Mid-German Crystalline Rise west of the River Rhine. Geol Rundsch 85:761–774

Reischmann T, Anthes G, Jaeckel P, Altenberger U (2001) Age and origin of the Böllsteiner Odenwald. Mineral Petrol 72:29–44

Renne PR, Mundil R, Balco G, Min K, Ludwig KR (2010) Joint determination of ^{40}K decay constants and ^{40}Ar*/^{40}K for the Fish Canyon sanidine standard, and improved accuracy for ^{40}Ar/^{39}Ar geochronology. Geochim Cosmochim Acta 74:5349–5367

Scherer EE, Mezger K, Münker C (2002) Lu–Hf ages of high-pressure metamorphism in the Variscan fold belt of southern Germany. Geochim Cosmochim Acta Suppl 66:A677

Schubert W, Lippolt HJ, Schwarz W (2001) Early to Middle Carboniferous hornblende ^{40}Ar/^{39}Ar ages of amphibolites and gabbros from the Bergsträsser Odenwald. Mineral Petrol 72:113–132

Schulz B (2013) Monazite EMP–Th–U–Pb age pattern in Variscan metamorphic units in the Armorican Massif (Brittany, France). Z Dt Ges Geowiss 164:313–335

Schulz B, Schüssler U (2013) Electron-microprobe Th–U–Pb monazite dating in Early Paleozoic high-grade gneisses as a completion of U–Pb isotopic ages (Wilson Terrane, Antarctica). Lithos 175–176:178–192

Schulz B, von Raumer JF (2011) Discovery of Ordovician–Silurian metamorphic monazite in garnet metapelites of the Alpine External Aiguilles Rouges Massif. Swiss J Geosci 104:67–79

Siebel W, Eroglu S, Shang CK, Rohrmüller J (2012) Zircon geochronology, elemental and Sr–Nd isotope geochemistry of two Variscan granitoids from the Odenwald–Spessart crystalline complex (Mid-German Crystalline Rise). Mineral Petrol 105:187–200

Sommermann AE (1993) Zirkonalter aus dem Granit der Bohrung Saar 1. Beiheft Eur J Mineral 5:145

Spear FS (2010) Monazite-allanite phase relations in metapelites. Chem Geol 279:55–62

Spear FS, Pyle JM (2002) Apatite, monazite and xenotime in metamorphic rocks. In: Kohn M, Rakovan J, Hughes JM (eds) Phosphates—geochemical, geobiological and materials importance. Rev Mineral Geochem 48:293–335

Spear FS, Pyle JM, Cherniak D (2009) Limitations of chemical dating of monazite. Chem Geol 266:218–230

Stampfli GM, Hochard C, Vérard C, Wilhem C, von Raumer J (2013) The geodynamics of Pangea formation. Tectonophysics 593:1–19

Stephan T, Kroner U, Hahn T, Hallas P, Heuse T (2016) Fold/cleavage relationships as indicator for late Variscan sinistral transpression at the Rheno-Hercynian–Saxo-Thuringian boundary zone, Central European Variscides. Tectonophysics 681:250–262

Suzuki K, Kato T (2008) CHIME dating of monazite, xenotime, zircon and polycrase: protocol, pitfalls and chemical criterion of possible discordant age data. Gondwana Res 14:569–586

Suzuki K, Adachi M, Kajizuka I (1994) Electron microprobe observations of Pb diffusion in metamorphosed detrital monazites. Earth Planet Sci Lett 128:391–405

Todt WA, Altenberger U, von Raumer JF (1995) U–Pb data on zircons for the thermal peak of metamorphism in the Variscan Odenwald, Germany. Geol Rundsch 84:466–472

Villaseca C, Castiñeiras P, Orejana D (2015) Early Ordovician metabasites from the Spanish Central System: a remnant of intraplate HP rocks in the Central Iberian Zone. Gondwana Res 27:392–409

von Raumer JF (1973) Die mineralfazielle Stellung der Metapelite und Metagrauwacken zwischen Heppenheim und Reichelsheim (Odenwald). N Jb Mineral Abh 118:313–336

von Raumer JF, Stampfli GM (2008) The birth of the Rheic Ocean—Early Palaeozoic subsidence patterns and subsequent tectonic plate scenarios. Tectonophysics 461:9–20

von Raumer JF, Stampfli GM, Arenas R, Sánchez Martínez S (2015) Ediacaran to Cambrian oceanic rocks of the Gondwana margin and their tectonic interpretation. Int J Earth Sci 104:1107–1121

von Seckendorff V, Timmermann MJ, Kramer MJ, Wrobel P (2004) New ^{40}Ar/^{39}Ar ages and geochemistry of late Carboniferous-early Permian lamprophyres and related volcanic rocks in the Saxothuringian Zone of the Variscan Orogeny (Germany). In: Wilson M, Neumann E-R, Davies GR, Timmermann MJ, Heeremans M, Larsen BT (eds) Permo-Carboniferous magmatism and rifting in Europe. Geol Soc Lond Spec Publ 223:335–359

Weber K (1995) Structure of the Spessart crystalline complex. In: Dallmeyer RD, Franke W, Weber K (eds) Pre-Permian geology of Central and Eastern Europe. Springer, Berlin, pp 167–173

Will TM (1998) Phase diagrams and their application to determine pressure-temperature paths of metamorphic rocks. N Jb Mineral Abh 174:103–130

Will TM (2001) Paleostress-tensor analysis of late deformation events in the Odenwald Crystalline Complex and comparison with other units of the Mid-German Crystalline Rise, Germany. Mineral Petrol 72:229–247

Will TM, Schmädicke E (2001) A first report of retrogressed eclogites in the Odenwald Crystalline Complex: evidence for high-pressure metamorphism in the Mid-German Crystalline Rise, Germany. Lithos 59:109–125

Will TM, Schmädicke E (2003) Isobaric cooling and anti-clockwise P–T paths in the Variscan Odenwald Crystalline Complex. J Metamorph Geol 21:469–480

Will TM, Lee S-H, Schmädicke E, Frimmel HE, Okrusch M (2015) Variscan terrane boundaries in the Odenwald–Spessart basement, Mid-German Crystalline Zone: new evidence from ocean ridge, intraplate and arc-derived metabasaltic rocks. Lithos 220–223:23–42

Williams ML, Jercinovic MJ, Goncalves P, Mahan K (2006) Format and philosophy for collecting, compiling, and reporting microprobe monazite ages. Chem Geol 225:1–15

Zeh A (1996) Die Druck-Temperatur-Deformationsentwicklung des Ruhlaer Kristallins (Mitteldeutsche Kristallinzone). Geotekt Forsch 86:1–214

Zeh A, Gerdes A (2010) Baltica- and Gondwana-derived sediments in the Mid-German Crystalline Rise (Central Europe): implications for the closure of the Rheic ocean. Gondwana Res 17:254–263

Zeh A, Will TM (2010) The Mid-German Crystalline Rise. In: Linnemann U, Romer RL (eds) Pre-Mesozoic geology of Saxo-Thuringia–From the Cadomian active margin to the Variscan orogen. Schweizerbart, Stuttgart, pp 195–220